STATE UNIVERSITY OF NEW YORK AT STONY BROOK

COLLEGE OF ENGINEERING

Report No. 223

ON PURE BENDING OF FERROCEMENT BEAMS

by

F. P. Chiang

and

N. Thiruvillakatt

Department of Mechanics
College of Engineering
State University of New York
Stony Brook, New York 11790

March 1972

On Pure Bending of Ferrocernent Beams

by

F.P. Chiang, Associate Professor

and

N. Thiruvillakatt, Graduate Student

Dept. of Mechanics, College of Engineering
State University of N.Y. at Stony Brook

Report No.
223

March 1972

ABSTRACT

A series of tests was conducted on ferro-cement beams which were identical in size, weight, and quantity of wire mesh reinforcement but varied in the placement of the reioforcement.. Four different reinforcement placement configurations were tested and it was found that the strongest beam was that with the reinforcement concentrated towards the outside surfaces of the beam. The beams were found to behave elastically within only a small range of bending strengths and then to deform plastically. The ultimate load and the neutral axis of the beam after yielding can be fairly accurately predicted using conventional reinforced concrete theory.

ACKNOWLEDGEMENTS

The authors would like to thank Mr. Whitby K. Ellsworth of Samson Marine Design Enterprises of Long Island, Inc. who introduced the authors to the interesting field of ferro-cement and provided financial support of the research work reported here. His personal involvement in the course of the study from critical discussion to physical construction of the beams contributed invaluably to the progress of the project.

Mr. A.K. Narasimham, a former graduate student of the Dept. of Mechanics was involved in the early stages of the investigation. He helped in constructing the beams and carrying out the tests. The authors are happy to acknowledge his contribution.

The authors also wish to most gratefully acknowledge the support of the G.F. Wright Steel and Wire Company of Worcester, Massachusetts and especially of Mr. George Booth, the Product Sales Manager, who provided both the wire mesh used in the project and the technical assistance related to their product. They were especially helpful in modifing their manufacturing process to provide us with a special material which is felt will make boat construction easier without any strength loss.

INTRODUCTION

Ferro-cement consists of cement mortar as matrix and several layers of wire mesh as reinforcement. One of the important advantages of this material is the possibility of constructing thin structures, having relatively high tensile strength. In the case of conventional reinforced concrete, cracks appear even for relatively small deformations whereas in ferro-cement visible cracks appear only after considerable deformation. In addition, the material is relatively easy and inexpensive to manufacture. These unique features of ferro-cement make it an attractive material for building domes, shells, boats, etc. Thoughthere is sufficient practical knowledge available to permit the construction of ferro-cement structures, the properties and behavior of the material are not yet fully understood.

Dr. Pier Luigi Nervi, the famous Italian architect demonstrated conclusively for the first time in the 1940's that ferro-cement can be advantageously used for building boats and other structures. (1)+. Since then, much research has been carried out to assess the properties and behavior of ferro-cement. Extensive investigations were carried out by V.F. Bezukladov (2) and others of the U.S.S.R.

They have introduced the relationship between the crack formation and the specific surface of reinforcement.* Lyon D.G. Collen (3) of Ireland conducted experiments on ferro-cement beams and found that the ultimate bending stresses vary linearly with the steel content in the beam. He considered ferro-cement as a homogenous material and no attempt was made to determine the effect of the location of reinforcement on the ultimate bending stresses. Hans Frederick Muhlert (4) used the R.C. beams theory to predict the ultimate strength of ferro-cement beams. S.P. Shah (5) (6) calls ferro-cement a quasi "crack-free, homogenous" material. He attempted to relate the specific surface of reinforcement to the "stress at first crack." Romualdi and Batson (7) (8) discuss the crack arrest mechanism and the effect of closely spaced wire reinforcement on the ultimate capacity of the beams. The report published by the Canadian Fisheries (9) gives a very good comprehensive view of the subject as well as a list of most of the published works.

The usual assumption that ferro-cement behaves like a homogenous material has not been fully supported with experimental evidence, nor has it been repudiated. The purpose of this research is to determine the behavior of ferro-cement beams in pure bending. The results obtained from this research lead us to believe that ferro-cement behaves like a homogenous material only in a limited range, and beyond that it behaves quite similarly to the conventional reinforced concrete.

*Specific surface is defined as the bond area of reinforcement per unit volume of composite.

+Numbers in the parenthesis denote the references at the end of the paper.

DETAILS OF THE SPECIMENS

All the specimens tested were of the same size and contained identical amounts of reinforcernent. The bond area between the reinforcement and mortar was consequently also the same for all specimens. But the location of reinforcernent across the thickness of the beams was varied for each of four different configurations.

Each beam was 30" long, 6" wide and 1" thick. The ratio of cement, sand, and water in the mortar was 1 to 1: 5 to 0: 4 respectively, by weight. The cube strength of the mortar was found to be about 8000 psi at 28 days water cure. Six layers of woven, ungalvanized wire mesh were used in all the beams, the size of the mesh being 0.25" x 0.25", 23 gage. The percentage of reinforcement was by 1./$ weight. The ultimate tensil strength of the wire strand used in the reinforcement was 160,000 to 170,000 psi.

A constant cover of 1/8" of mortar over the exterior layers of reinforcement was provided for all beams. The curing period was 28 days, immersed in water.

Four different configurations of beams were constructed with only the reinforcement location varying. (Fig.1). Three beams of each configuration were fabricated. The four configurations are:

TYPE A Six layers of wire meshes were uniformly distributed across the thickness of the beam (Fig. 1A).

TYPE B Two layers each at top and bottom and one layer each between the middle plane of the beam and extreme layers of reinforcement (Fig. 1B).

TYPE C Two layers each at top, bottom and middle (Fig. 1C).

TYPE D Three layers each at top and bottom (Fig. 1D).

EXPERIMENTAL SET UP

All the beams were tested for their behavior in pure bending. The beam was supported at its' ends, with an effective span of 27" and equal loads were applied at 6" from either support. The bending moment diagram and shear force diagram are as shown in Fig. 2. It is clear from the figure that the region between A and B is experiencing

a pure bending moment without any shear force. Maximum bending moment= P/2 x 6=3P inch pounds, where P=applied load.

Strain gages were attached to the top and bottom surfaces at the center of the beam and strains were read directly from the strain indicator. Deflection was measured by means of six dial gages along the span of the beam. Strain gage readings and deflection mcasurernents were taken for every 30 to 40 pounds for small loading and at every 60 pounds for larger loadings.

TESTING OF BEAMS

The three samples of each beam type were subject to: 1) 300 pounds loading; 2) 600 pounds loading, then release of the load, then reloading to failure; 3) and direct loading to failure. See Table I.

1. 300 POUNDS LOADING One beam from each type (A I, BI, CI, and DI) were loaded to 300 pounds. When the load was released, very small permanent strains and deflections were observed. The extreme tensile fiber strain was slightly higher then the extreme compressive fiber strain for the same load. Figure 3 shows the variation of the strain of the extreme tensile fiber to the load.

2. 600 POUNDS LOADING AND RELOADING TO FAILURE In this case, one beam from each types A, 6, and C and two beams from type D were loaded to 600 pounds initially. When the load was released, large amounts of permanent deflection and strain were observed. These beams were again loaded to their ultimate capacity. The strain of the extreme tension fibers, when the load approached the failure value, was so large that it could not be measured in the strain indicator for types A, B, and C. Type D had relatively small failure strains of the extreme tensile fiber, and was measured until the beam failed. The figures 4, 5, and 6 show the relation between fiber strains and load, and deflection and load.

3. DIRECT LOADING TO FAILURE One beam each from types A, B, and C were directly loaded to failure. The ultimate strains were so large that it could not be measured in the strain indicator. Fig. 7 shows the relation between the tensile and compressive fiber strains and the load.

ANALYSIS OF EXPERIMENTAL DATA

For a direct load up to-330 pounds, it is observed from figures 4, through 7, that there is a linear relationship between the strain

and load as well as deflection and load. Beyond this load the variation is non-linear. This load at which the linear variation changes to non-linear can be considered as the load at which micro-cracks start forming at the extreme tension fiber. (These cracks are not visible to the naked eye.) This linear variation of strain with load and deflections with load is observed only in the case of direct loading. When the cracked beams were unloaded and re-loaded, the strains and central deflections vary non-linearly with the load. Type D had relatively small ultimate tensile strain.

Of the four types of beams, type D has shown higher ultimate strength (see Table I) and high resistance to deformation and deflection. In addition, regardless of the type of beam or nature of loading, the compressive fiber strains were found to be much smaller than the tensile fiber strains (Fig. 7). According to elastic beam theory, the strains of compressive fiber and tensile fiber should be equal since the neutral axis lies in the middle of the beams. Had the beams been behaving like a homogenous material, all the beams should be expected to behave identically since the amount and bond area of reinforcement are same in all the beams.

CLASSICAL BEAMS THEORY

According to this theory the neutral axis lies at the middle of the beam section. The region below the neutral axis is subjected to tensile stresses while the region above neutral axis is subjected to compressive stresses. The stress distribution is linear across the section as shown in figure 8(a). Since the neutral axis lies in the middle, the extreme fibers are subjected to the same magnitude of stresses. The extreme fiber stresses, for a given bending moment, are given by

$$ft = fc = \frac{M\ d/2}{I}$$

Where: M=applied bending moment

ft, fc=extreme tensile and compressive fiber stresses respectively

d=depth of the beam

I=Moment of Inertia of the beam section

$=\frac{bd}{12}$ where b=width of beam

The applied bending moment should balance the resisting moment of the beam section.

Resisting Moment=Area of stress diagram (compressive or tensile) x lever arm, where lever arm is the distance between the centers of compressive and tensile stress diagrams.

For a linearly elastic material, the stress is directly proportional to strain. Hence the strains of the extreme fibers must be equal. Since ferro-cement is not a homogenous material, the neutral axis. does not lie in the middle plane of the beam, and hence the compressive and tensile fiber strains are different. It is difficult to ascertain the nature of stress distribution across the beam section unless the location of the neutral axis is predetermined. Moreover, the stresses may not vary linearly across the beam section, since ferro-cement is neither a homogenous material nor perfectly elastic. But it can be reasonably assumed that the strains vary linearly across the beam section. The location of neutral axis can be determined from the extreme fiber strains. (Fig. 8 (b)).

$$\frac{Es}{Ee} = \frac{d-n}{n}$$

$$n + \frac{dEe}{Es + Ee}$$

Where n=distance of neutral axis from top of beam

Ee=compressive fiber staain

Es=tensile fiber strain

d=depth of the beam

The neutral axis was thus calculated for different strain measurements. Fig, 9 shows the positions of neutral axis as the load increases. Below the cracked range, for a load of about 330 pounds, the neutral axis is found to lie very near the middle plane of the beam, indicating homogenous behavior of this material for this range of loading. (Before the crack formation, the mortar and steel act together like a homogenous material.) But as the load increases further, the neutral axis jumps up towards the top of the beam. This corresponds to the crack formation and subsequent crack propagation in the tensile region of the beam. Due to the crack formation, the mortar becomes ineffective to take any further stresses and the stress is transferred to the reinforcement. Since the resisting moment should balance the applied bending moment, the neutral axis shifts up to a new position. This theory is in conformity

with the conventional reinforced concrete beam theory.

R.C. Beam Theory: According to this theory, the steel in the tension side is assumed to carry the complete tensile stresses. The neutral axis is calculated from the principle of "equivalent steel area", which is based on the theory that the strains in the steel and concrete are equal. (Fig. 8 (c))

. From the Figure 8 (c):

Taking moments of areas (in the stress diagram) about the neutral axis,

$$m\,As\,(d_1-n) = b \times n \times \frac{n}{2}$$

Where $m = \frac{Es}{Ee}$ = $\frac{\text{Young's modulus of steel}}{\text{Young's modulus of concrete}}$

b=width of beam

d_1=effective depth of beam

n=neutral axis position, from the top of beam

Hence 'n' can be calculated.

The moment of resistance of the beam section is

$$M\text{-}R = As \times fs \times Jd_1$$

Where As=Area of steel

fs=Stress in steel

Jd_1=lever arm

Assuming a value of m=10, the neutral axis was calculated for the four types of beams. This value is found to be 0.23" (from the top of the beam) for all types of beams. This value almost concurs with the value of neutral axis obtained from the strains for ultimate loads.

An attempt is made to theoretically calculate the ultimate capacity of the beams from the ultimate stress theory of R-C beams. The steel in the tension region, irrespective of its location, is assumed to be fully stretched, while the mortar is assumed to carry no load. The location of neutral axis is taken on 0.24" from the top of the beam, and the center of compression stress diagram is taken as 0.1" from top in all cases. (Fig.10 (a) to 10 (d)). Each layer of mesh consists of 22 wires of 0.025" diameter. The maximum capacity of one layer is

$$22 \times \frac{\pi}{4} \quad (0.025)^2 \times 170{,}000 = 1840 \text{ pounds.}$$

TYPE A: Fig. 10 (a)

Taking moments of steel stresses ft_1, ft_2, ft_3, etc. about the center of compression stress,

Moment of resistance=1840 (0.775+0.625+0.475+0.325+0.175)

=5074 inch pounds

Maximum applied bending moment at failure=4284 inch pounds (From the Table I)

Similarly for

TYPE B: Fig 10 (b)

Moment of resistance=1840 (2x0.775 + 0.588 + 0.213)

=4300 inch pounds

Maximum applied bending moment at failure-4644 inch pounds

TYPE C: Fig. 10 (c)

Moment of resistance=1840 (2x0.775= 2 x 0.4)

=4320 inch pounds

Maximum applied bending moment at failure=4338 inch pounds

TYPE D: Fig. 10 (d)

Moment of resistance=1840 (3x0.775)

=4270 inch pounds

Maximum applied bending moment at failure=5115 inch pounds

In the above cases it is seen that the actual capacities of the beams are greater than the calculated values except Type A.

In the above calculations, the stress in the mortar in the tension side is completely neglected. It is true, of course, that the mortar also carries a small amount of load, although the exact nature and amount of stress in the mortar cannot be easily ascertained.

It is also assumed that all the steels in the tension side are fully stretched irrespective of their location; this is not true. It can be easily seen that the steel near the neutral axis in the tension side is not fuliy stretched, since the strain at neutral axis is zero. In the case of type 'D' it can be reasonably assumed that all the three layers of reinforcement are fully stretched, while in the other types, the failure occurs even before the steel near the neutral axis is fully stretched. The higher capacity of type D can be explained by the above argument. In a more refined calculation, the positions of the steel should be included as a parameter.

CONCLUSIONS AND DISCUSSIONS

It is seen that for small range of stresses, the ferro-cement beams behave like a homogenous material. But since they are designed to operate for high stresses, the design procedure for a homogenous beams then can not be applied to ferro-cement. When the bending moment is about 1000 inch pounds (for which the extreme fiber stresses, according to classical beam theory is 1000 psi), microcracks start forming at the extreme fiber on the tension side. The cracks propagate inside the beam as the bending moment increases. These microcracks are not visible to the naked eye. Visible cracks appear only when the load approached to the ultimate values, which is in contrast with the conventional reinforced concrete, where the cracks appear even for very small tensile stresses.

The beams in type D have shown maximum resisting moment and therefore maximum resistance to strains and dcflections. Consequently, it seems advisable to concentrate the reinforcement in the extreme fibers of the ferro-cement beams. From the load-strain and load-deflection diagrams (Fig. 4,5,6, and 7) it is observed that the behavior of the beams are almost identical. Since the amount of steel used is very small (about 1.1% by weight), the differences in the behavior of the four types of beams are not expected to be large. A more pronounced difference would have resulted if the amount of reinforcement were larger.

Although more research is required for arriving at an exact design procedure of ferro-cement beams, sufficient informations have been obtained in this research to conclude that the ultimate capacity of the beam can be approximately determined from the ultimate stress theory of reinforcec concrete beams. The location of the neutral axis, for the cracked range can also be approximately determined from R-C beam theory. By applying a suitable factor of safety, the working loads for ferro-cement beams can be reasonably obtained, When the load is released at 600 pounds the micro-cracks in the mortar are closed since the steel, still in the elastic range, tries to attain its' original unstrained form. When the beam is loaded again, the cracks gradually widens up. Hence, while reloading the beams, the neutral axis gradually shifts up (Fig. 11), unlike a sudden shift of neutral axis in the case of direct loading (Fig. 9). it can be reasonably assumed that the mortar in the tension side also takes a part of the stress, even after cracks have been initiated.

Figures 12 and 13 are the typical curves of load vs. strain and load vs. central deflection. The behavior of any ferro-cement beam with a 1% steel content (by weight) can be expected to be identical. All the beams failed at the point of loading, indicating that the failure might have occured due to bending stresses as well as shear stresses. Further research is needed to establish the failure criterion.

REFERENCES

1) P.L. Nervi. "Ferro-cement-its' characteristics and potentialities" (In Italian) 1951

2) Bezukladov, V.F., K.K. Amelvanovich et al, "Ship Hulls Made of reinforced concrete". Translation from Russian Navalship Trans. No. 448, Nov. 1968

3) on D.G. Collen. "Some experiments in design and construction with ferro-cement". The Institution of Civil Engineers, Ireland, n . 1960

4) Hans Frederick Muhlert. "Analysis of Ferrocement in bending". Dept. of Naval Architecture and Marine Engineering, University of Michigan, Report No. 043, Jan. 1970

5) S.P. Shah "Ferrotement as a new Engineering Material". Report No. 70-11 University of Illinois at Chicago Circle Nov. 1970

6) S.P. Shah and Antoine E. Naaman "Mechanical properties of ferrocement" Research Report R 70-68. Dept. of Civil Engineering, Material Research Lab., School of Engineering, Massachusetts Institute of Technology, Cambridge, Mass. Sept. 1970

7) Romualdi, J.P., Batson, G.B., "Mechanics of crack arrest in concrete" Journal of the Engineering Mechanics division proceeding of the ASCE, June 1963

8) Romualde, J.P., Batson, G.B., "Behavior of reinforced concrete beams with closely spaced reinforcement" J. of the American Concrete Inst., June 1963

9) "Ferrocement for Canadian fishing vessels" Compiled and edited by W.H. Scott. Industrial Development Branch, Fisheries service. Dept, of Environment, Ottawa. Project Report No.42, Aug. 1971

LIST OF FIGURES

1) Configuration of reinforcement in the beams.

2) B.M. and shear force diagrams of the loaded beam.

3) Tensile Fiber Strain vs. load for 300 pounds loading.

4) Load vs. central deflection-Loading and Reloading.

5) Load vs. Tensile Fiber Strain-Loading and Reloading.

6) Load vs. Compressive Fiber Strains-Loading and Reloading.

7) Load vs. Tensile and Compressive Fiber Strains-Direct Loading.

8) a) Position of Neutral Axis according to beam theory.
b) Position of Neutral Axis calculated from fiber strains.
c) Position of Neutral Axis according to R.C. beam theory.

9) Neutral Axis vs. Load-Direct Loading.

10) Stress diagram across the section of the beams for calculating moment of resistance by ultimate stress theory of R.C. beams.

11) Neutral Axis vs. Load-Reloading.

12) Typical Curve-Load vs. Tensile Fiber Strain.

13) Typical Curve-Load vs. Central Deflection.

TABLE I

Beam Number	Beam Designation	Test No. 1	Test No.2	Test No.3* Maximum Load	Test No.4 Maximum Load	Beam Configuration See Fig.1
1	A_1	300 pounds				
2	A_2		600 pounds	1346 pounds at failure		Type A
3	A_3				1510 pounds at failure	
4	B_1	300 pounds				
5	B_2		680 pounds	1575 pounds at failure		Type B
6	B_3				1520 pounds at failure	
7	C_1	300 pounds				
8	C_2		600 pounds	1478 pounds at failure		Type C
9	C_3				1414 pounds at failure	
10	D_1	300 pounds				
11	D_2		600 pounds	1470 pounds at failure		Type D
12	D_3		600 pounds	1640 pounds at failure		

*This the load at which the beam failed. However, failure modes indicated that there was contribution from sheer as well as from bending moment.

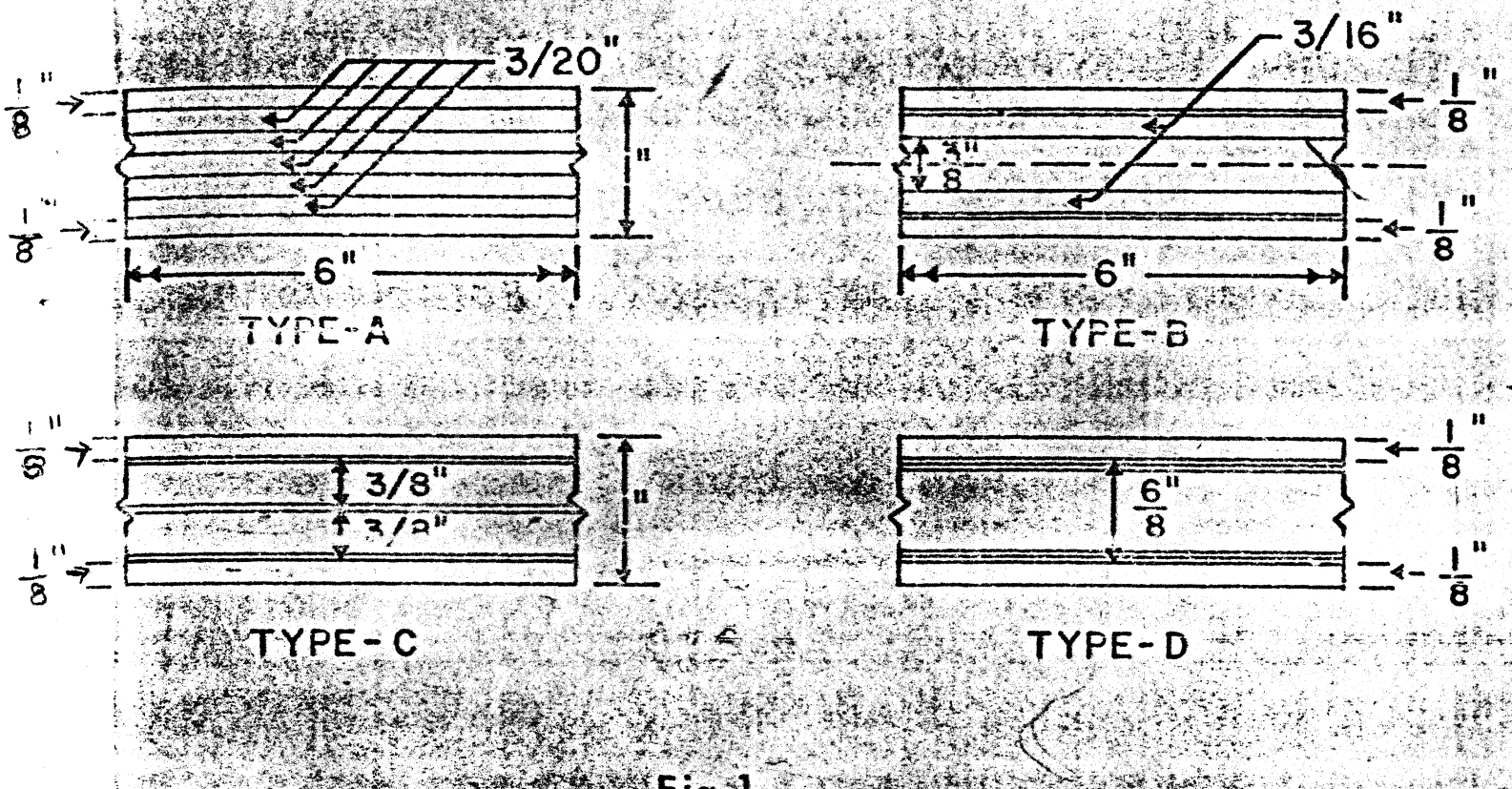

Fig 1

CLASSIFICATION OF BEAMS

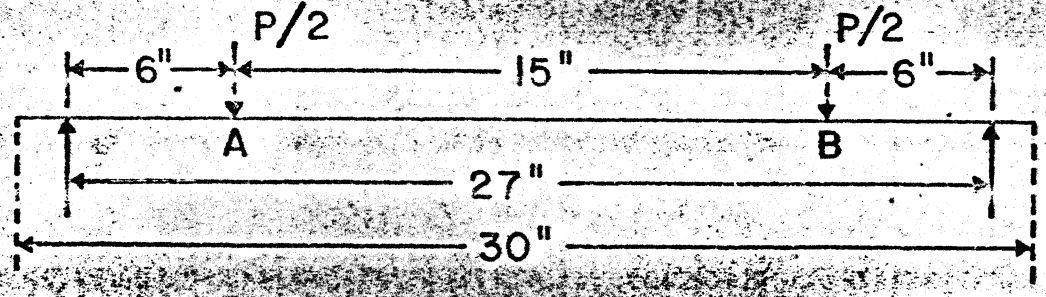

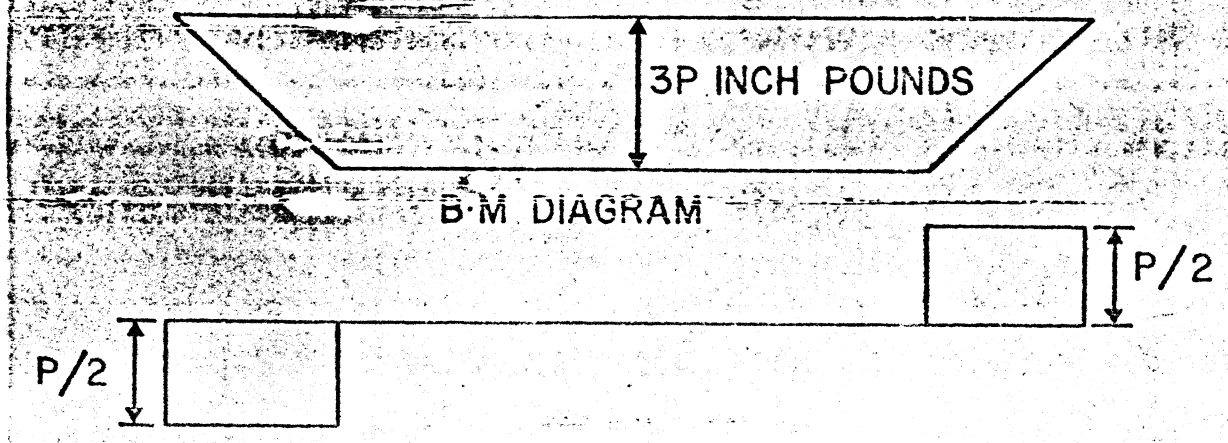

Fig 2

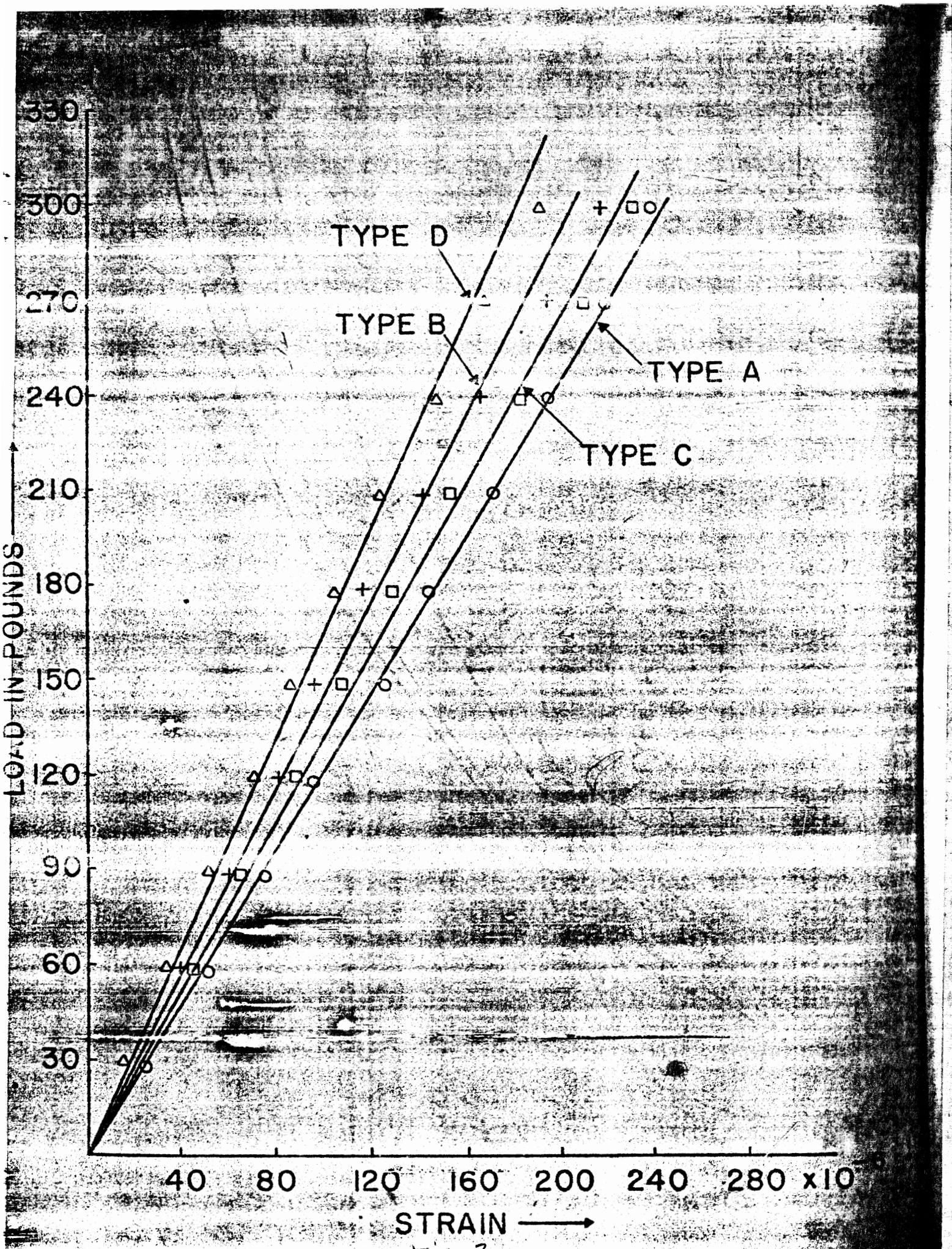
330
300
270
240
210
180
150
120
90
60
30
LOAD IN POUNDS
TYPE D
TYPE B
TYPE A
TYPE C
40
80
120
160
200
240
280 x10
STRAIN

Fig 3

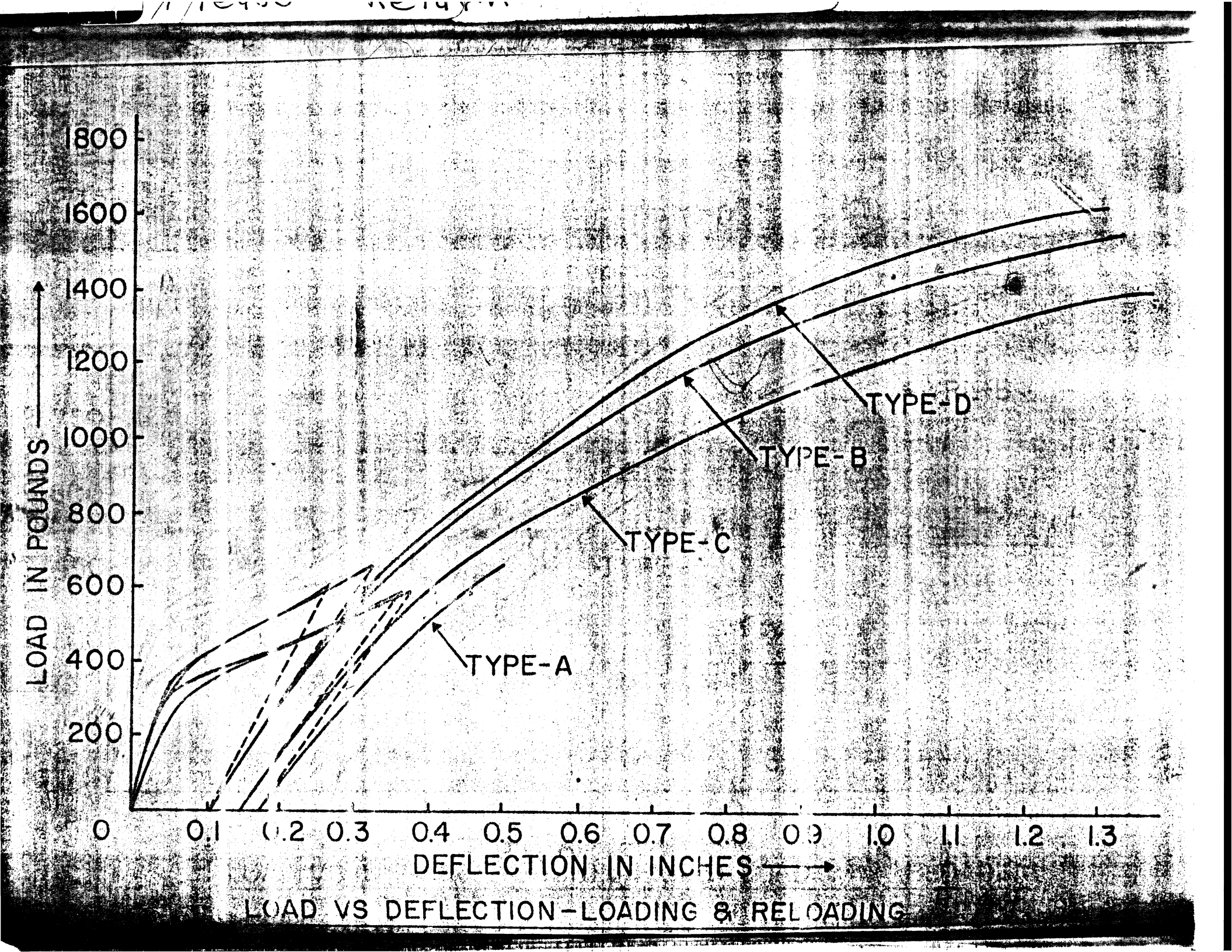

LOAD VS DEFLECTION-LOADING & RELOADING

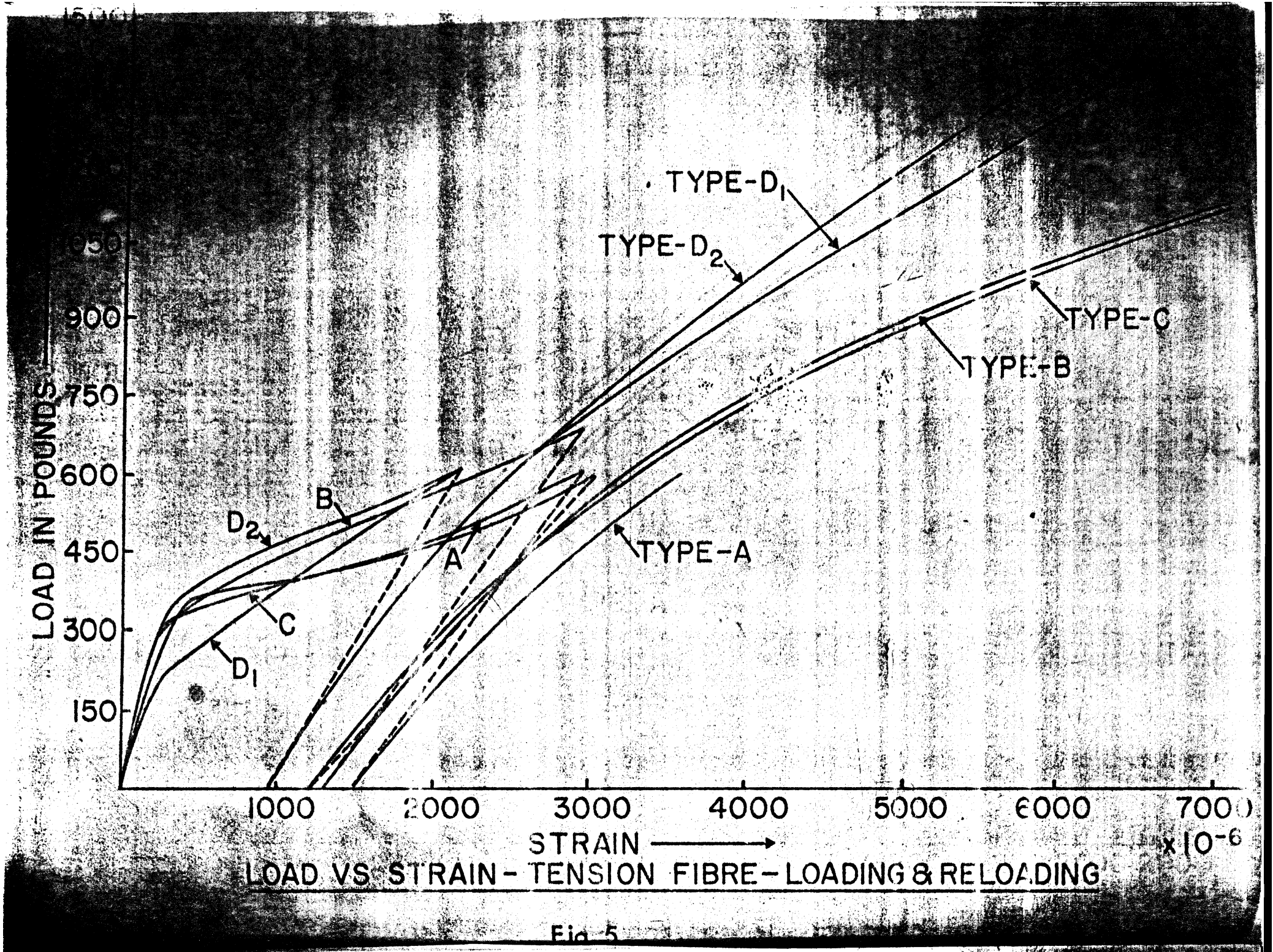

LOAD VS STRAIN - TENSION FIBRE - LOADING & RELOADING

Fig 5

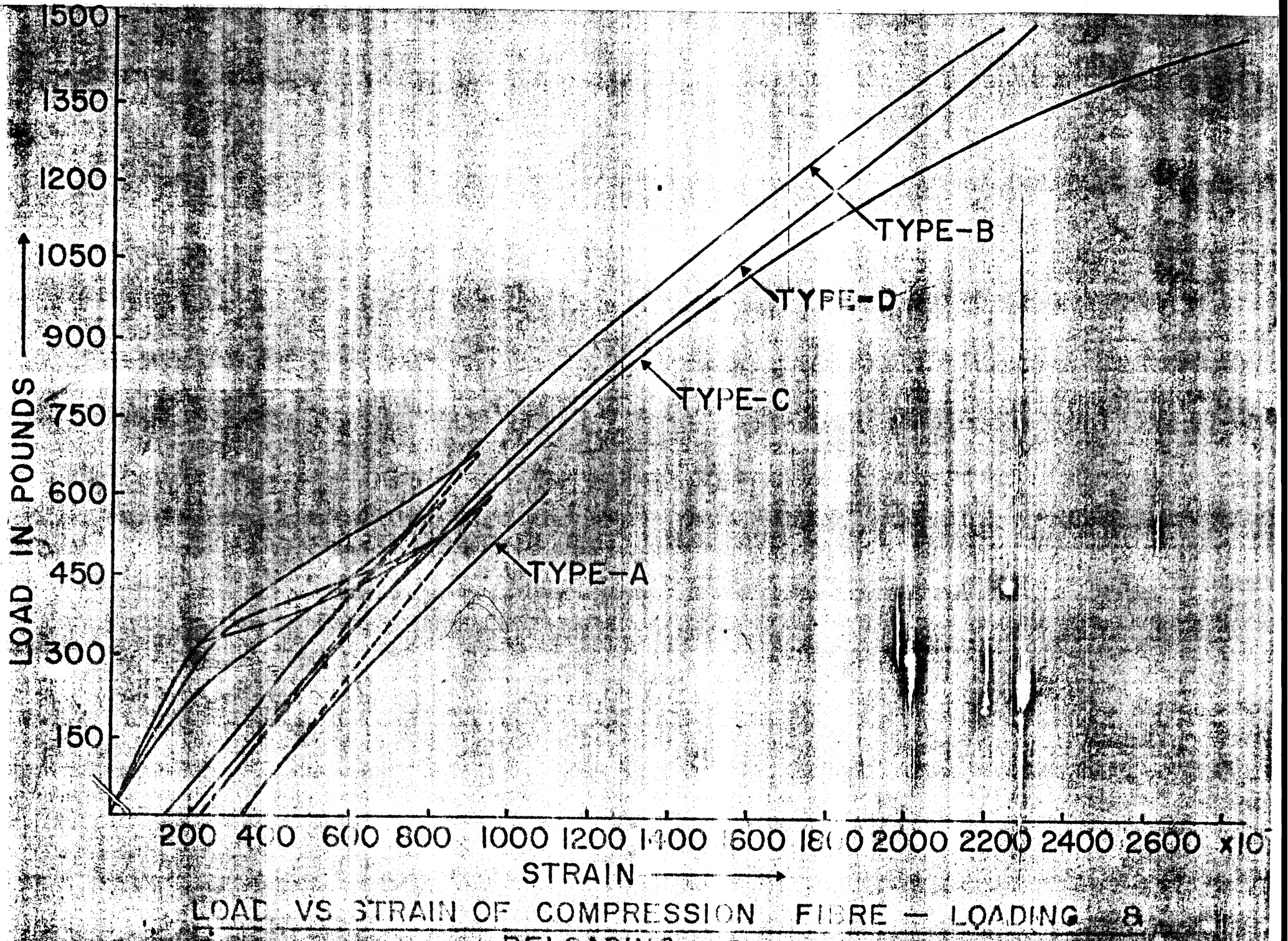

LOAD VS STRAIN OF COMPRESSION FIBRE — LOADING & RELOADING Fig 6

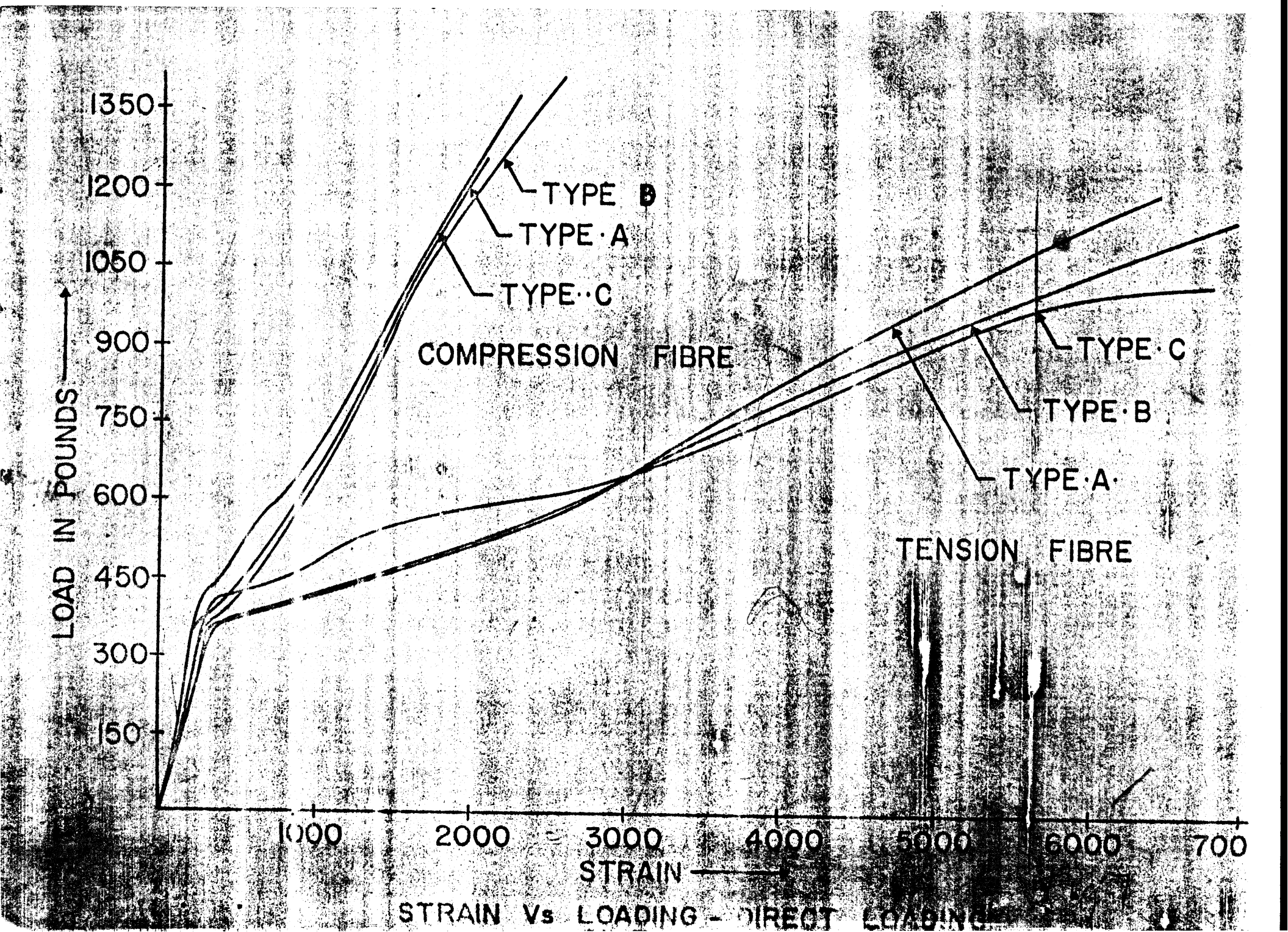
1350
1200
1050
900
750
600
450
300
150
LOAD IN POUNDS
TYPE B
TYPE·A
TYPE··C
COMPRESSION FIBRE
TYPE·C
TYPE·B
TYPE·A·
TENSION FIBRE
1000
2000
3000
4000
5000
6000
700
STRAIN
STRAIN Vs LOADING - DIRECT LOADING

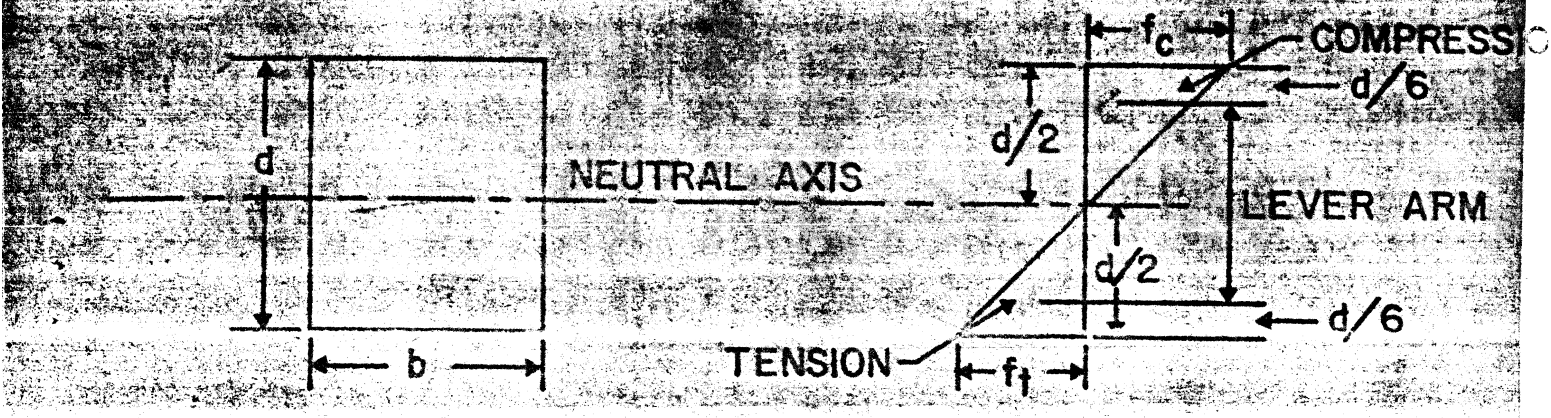

STRESS DIAGRAM

f_t , f_c = EXTREME FIBRE STRESSES

BEAM THEORY

Fig 8a

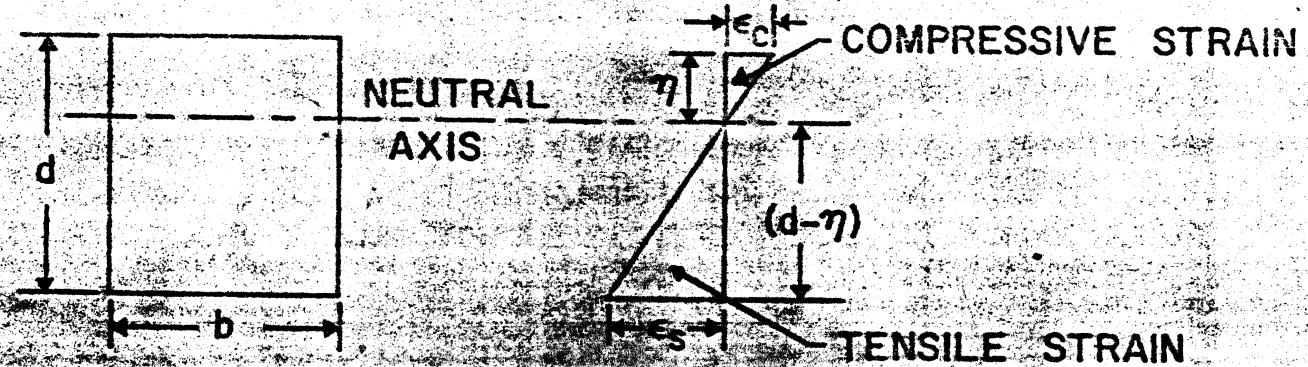

STRAIN DIAGRAM

ϵ_s , ϵ_c = EXTREME FIBRE STRAINS

$$\epsilon_s/\epsilon_c = \frac{(d-\eta)}{\eta} \qquad \eta = \frac{d\epsilon_c}{\epsilon_s+\epsilon_c}$$

CALCULATION OF N-A FROM FIBRE STRAINS

Fig 8b

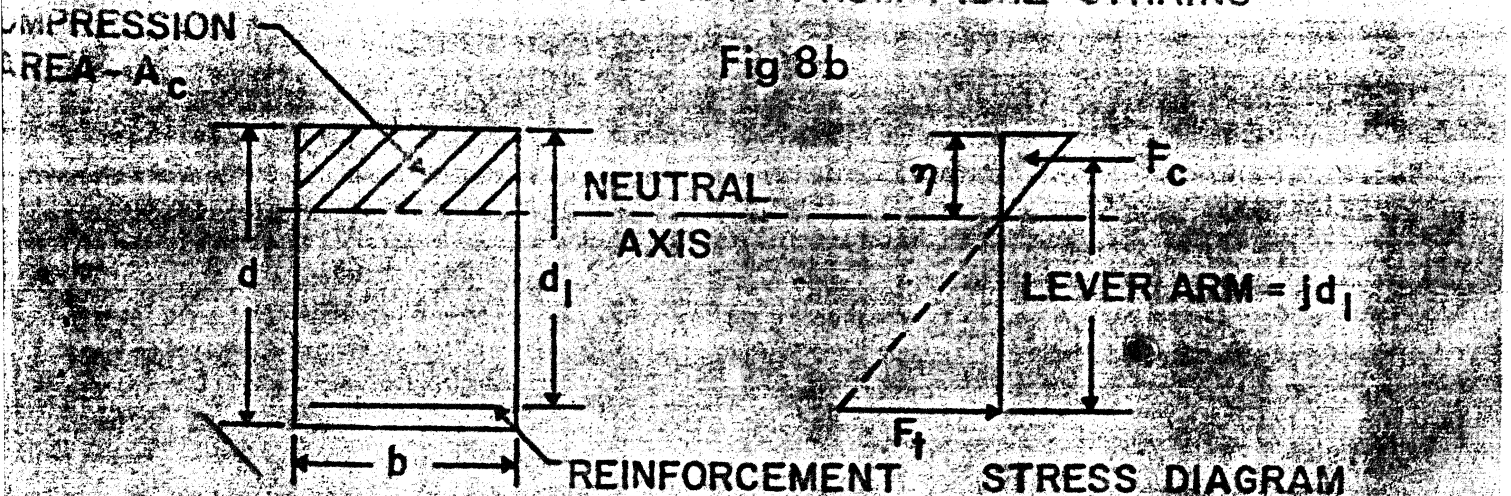

STRESS DIAGRAM

F_t = TOTAL TENSILE STRESS

F_c = TOTAL COMP. STRESS

R·C· BEAM THEORY

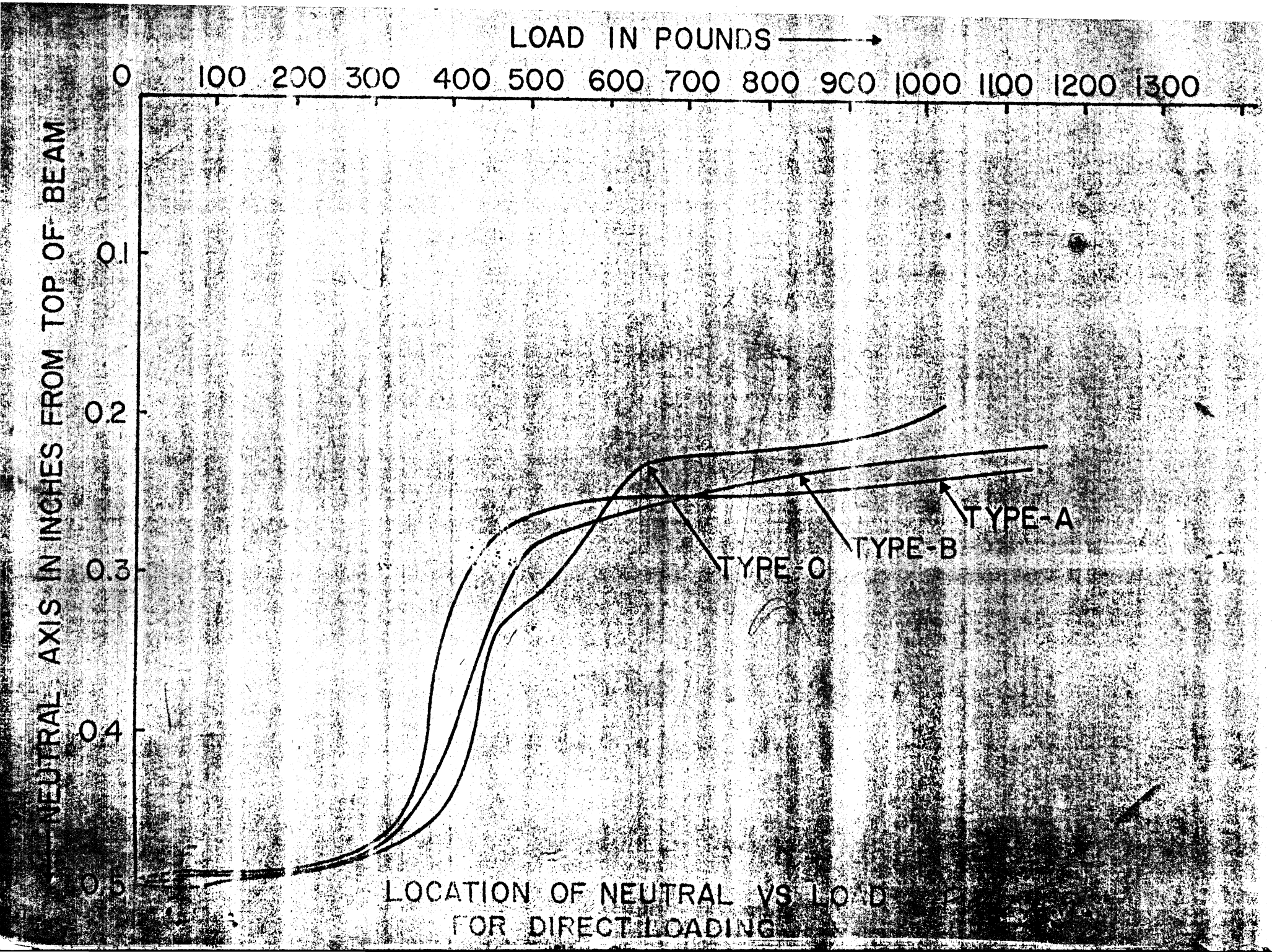

LOCATION OF NEUTRAL VS LOAD
FOR DIRECT LOADING

COMPRESSIVE STRESS

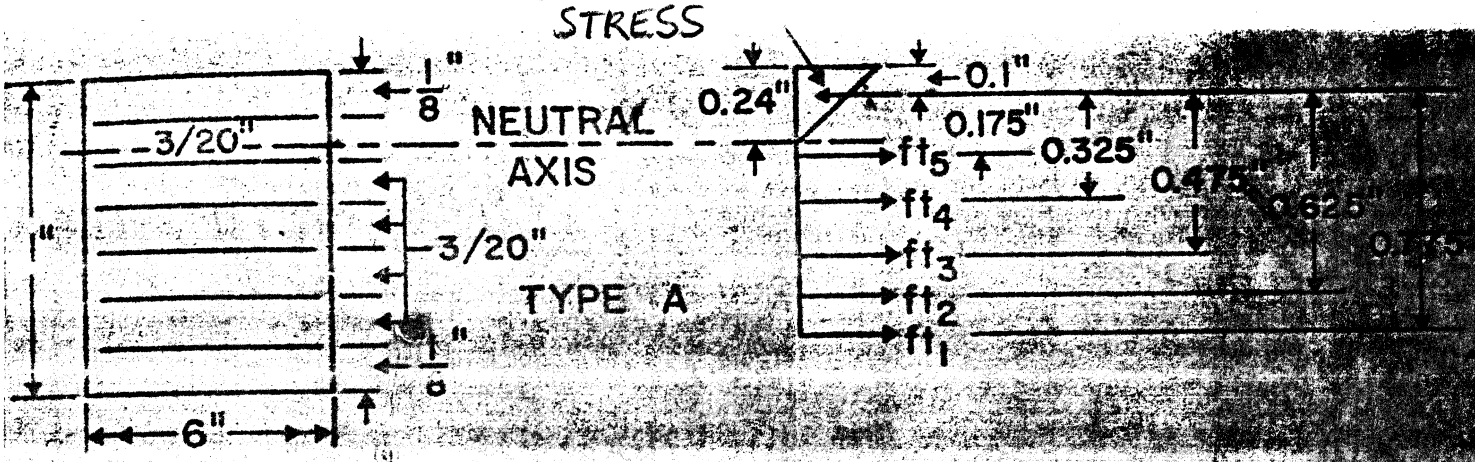

Fig 10a

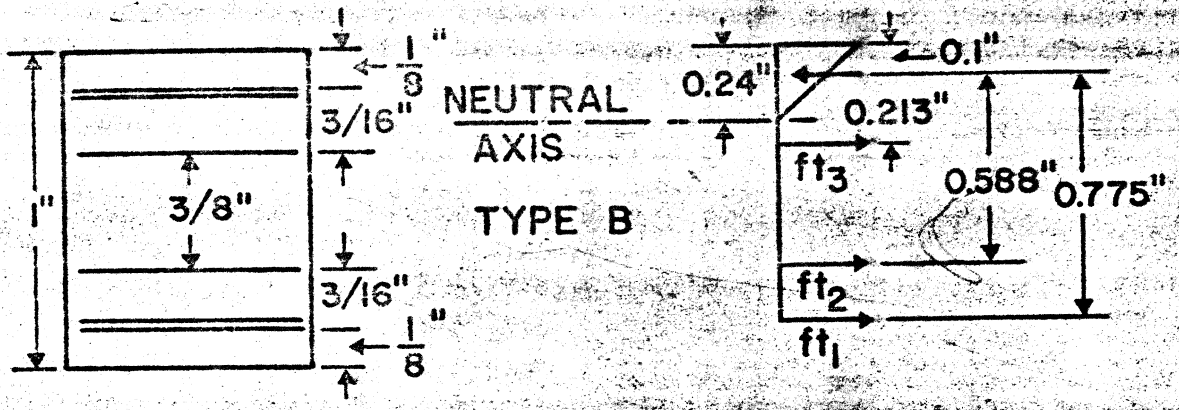

Fig 10b

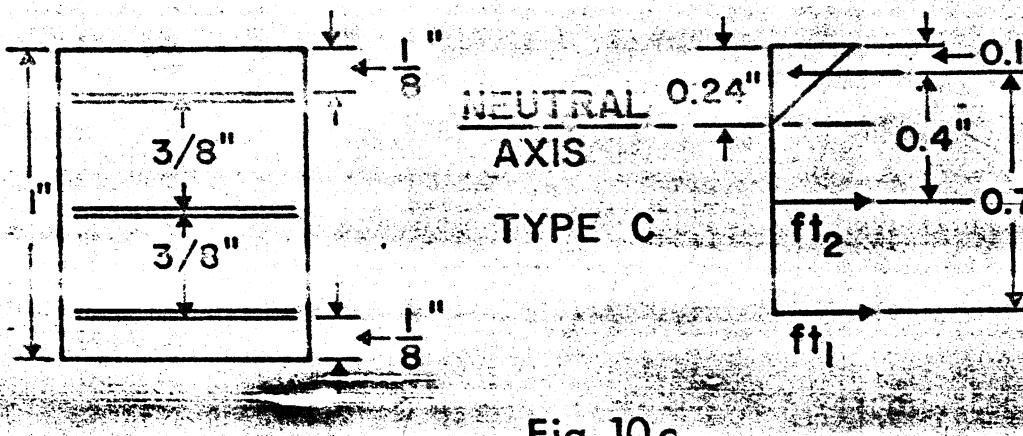

Fig 10c

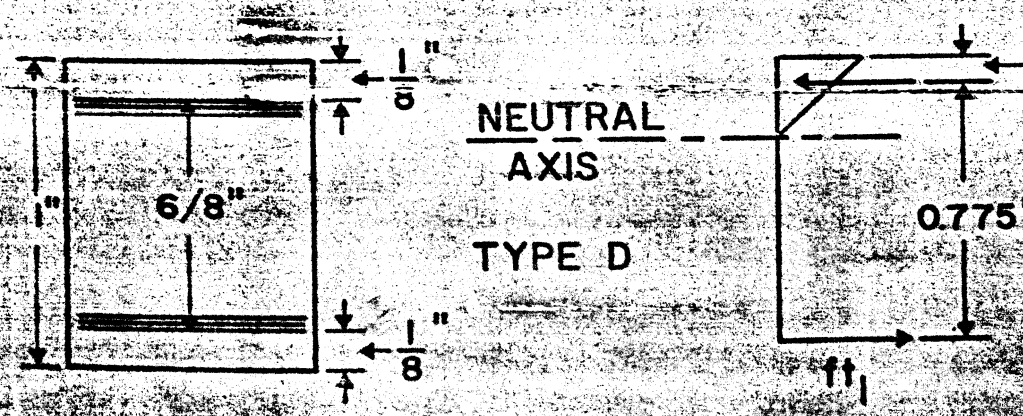

Fig 10d

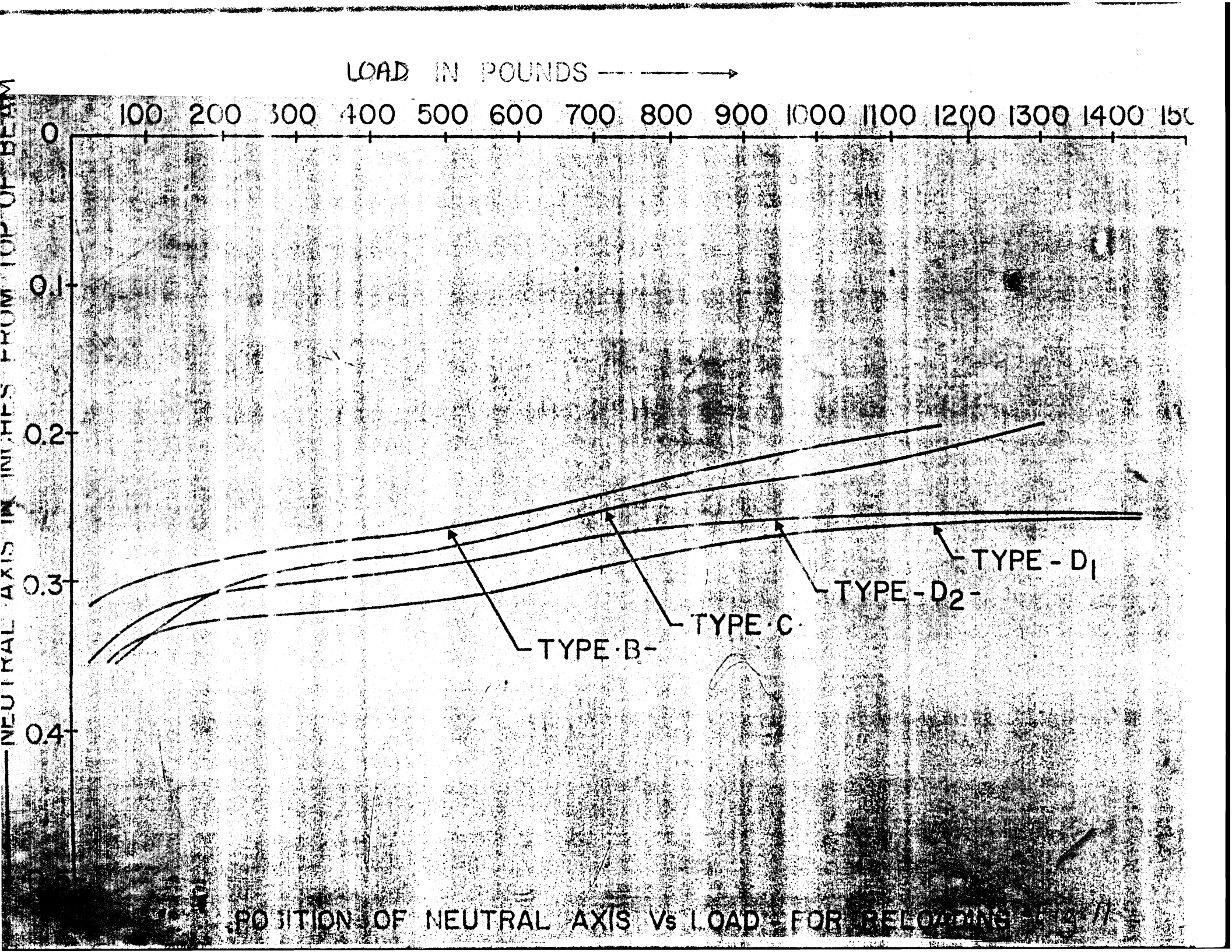

FIG. 11 - POSITION OF NEUTRAL AXIS Vs LOAD FOR RELOADING

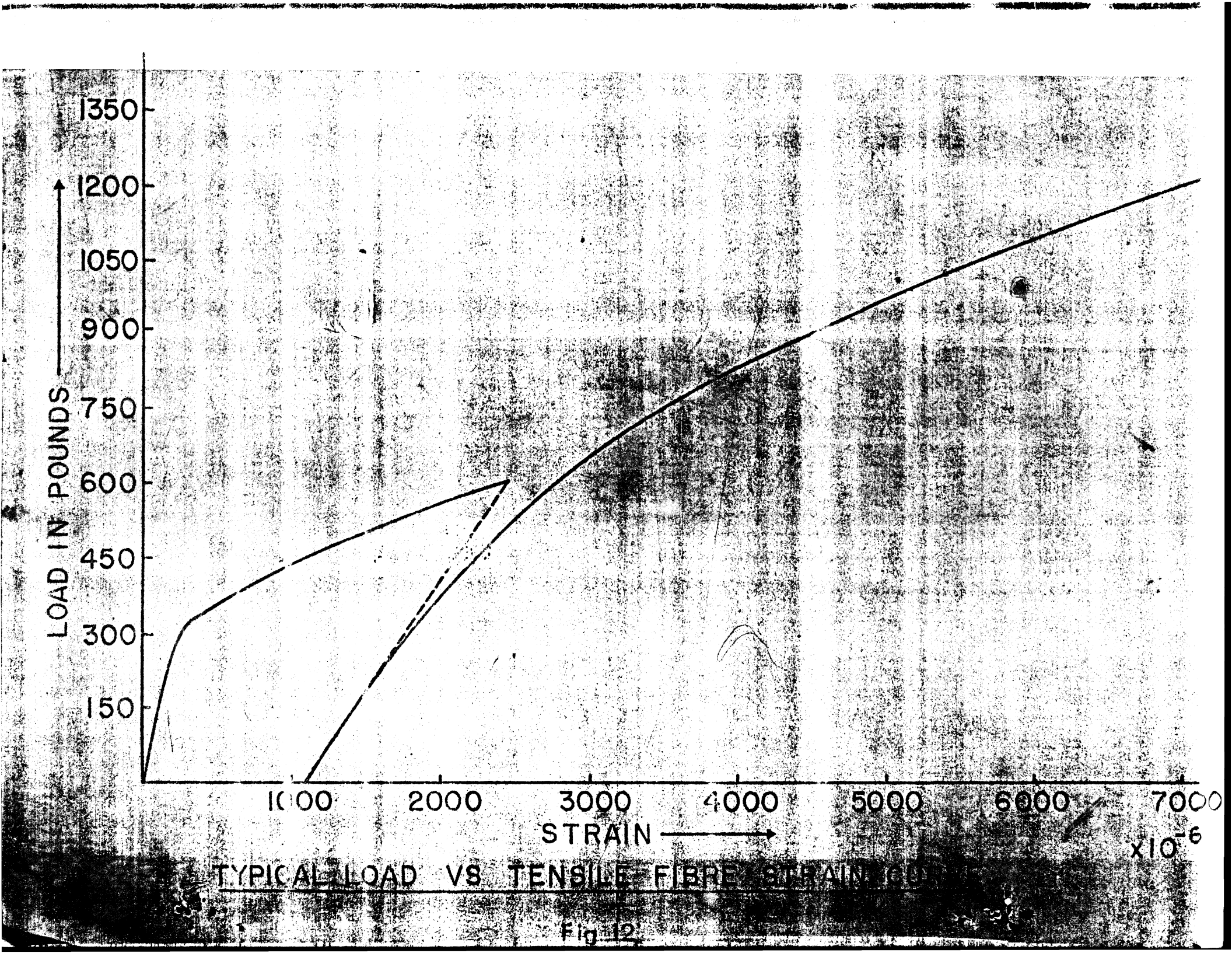

TYPICAL LOAD VS TENSILE FIBRE STRAIN CURVE

Fig 12